УДК 535.376

S. N. Svitasheva

Impact of Ti metallization and nitrogen plasma treatment on optical properties of Si-whiskers structures grown by MBE technique

Abstract

Spectroscopic ellipsometry measurements were employed to characterize nanowhisker structures grown by molecular-beam epitaxy on Si (111) substrates. Small clusters of gold deposited on the Si surface were used as the seeds for nanowhisker (NW) growth. Nitridation procedure was carried out for passivation to create ambient protection. Optical properties and thickness of passivation film were studied on satellite-speciment-speciment Si (111). By means of spectroscopic ellipsometry in the range of 1.5–4.77 eV, a) lateral optical inhomogeneity of the nanowhisker layer (NWL), b) substantial differing of optical properties of the NWL from those of single-crystal Si, and c) dependences of optical properties of the NWL on their length and on both metallization and nitridation procedure were revealed. Explanation of appearance in ellipsometric spectra of "«gigantic»" NWL absorption in the range of almost complete transparency of crystal Si was been suggested.

Key words: metamaterials, nanostructures, whiskers, optical properties, spectroscopic ellipsometry.

1. Introduction

Molecular-beam epitaxy growth of Si-NW have been reported lately [1–5] and remarkable progress has been achieved in the fabrication of whiskers with predefined radius, length, and position on the substrate. Reproducibility of the structural, electrical and optical properties of NWs is the key question for their application in various nanodevices.

The present study focuses on the optical properties of Si NW structures and on their transformation after passivation by deposited Ti metallic layer and after treatment in nitrogen plasma. The possibility to characterize NW structures by means of spectroscopic ellipsometry has been examined. We used the non-destructive, non-disturbing method of the spectroscopic ellipsometry for quantitative evaluation of the nanowhisker structures.

2. Experimental details

The Si-NW structures were grown by molecular-beam epitaxy. The substrates were Si (111) wafers. Successive treatments, that included a cleaning procedure, deposition of a 7 nm thick Si buffer layer at 200°C; deposition of a 100–150 nm thick Si buffer layer at 550°C, deposition of a 2 nm thick Au layer at 520°C, and growth of NWs (540 nm) at 550°C, were carried out *in situ*, inside the MBE system (UHV chamber RIBER SIVA 45). A detailed description of the growth procedure was given elsewhere [3]. As a result, Si whiskers with semispherical gold hats on their tops were fabricated.

It was revealed that the whiskers could inherit the Si crystal orientation but their composition was non-constant along length of the whisker [3, 5], and could include oxidized and eutectic layers.

From SEM studies the following parameters were found: the lengths of the NWs for first a set of structures were in the interval from 580 to 990 nm; the mean distances between them were 720–850 nm; and the NW diameters were from 200 to 70 nm; it is necessary to note that slim NWs have larger lengths. Volume fraction of whiskers in layer was about $6 \div 8\%$.

The other set of structures was grown with small lengths of whiskers such as following: 220 nm, 230 nm and 240 nm.

Optical properties of samples were studied by spectroscopic ellipsometry in the range of 1.5–4.77 eV using UVISEL ellipsometer (Jobin Yvon).

3. Results and discussion

As it is well known [11], the ellipsometry deals with ellipsometric angles Y and D which are related to the relative reflection coefficient r by expression (1):

$$\tan\Psi e^{i\Delta} = \frac{R_p(E)}{R_s(E)} \equiv \rho(E)\,, \qquad (1)$$

where, R_p *(E)* and R_s *(E)* are the Fresnel coefficients for p- and s- polarized light with photon energy *E*. In general case of stratified planar structures, when R_p and R_s depend upon parameters of all layers, of dielectric function of ambient medium, and of angle of light incidence j_0, ellipsometric spectra can be represented in terms of e_{pseudo} (E), if actual structure of sample was disregarded, and sample was accepted as semi-infinite homogeneous medium:

$$\varepsilon_{pseudo} = <\varepsilon_1> + <i\varepsilon_2> = \\ = \varepsilon_0 \tan^2\varphi_0 \left[1 - \frac{4\rho\sin^2\varphi_0}{(1+\rho)^2}\right]. \qquad (2)$$

Here, ε_1 and ε_2 are the real and imaginary parts of the pseudodielectric function, respectively. The ellipsometric spectra of the complex pseudodielectric function measured at several points on the wafer with NWs are shown in figure 1.

A clear correlation between ellipsometric spectra and whisker parameters was revealed. In the range of almost complete transparency of crystal Si (1.5–2.6 eV); the op-

tical properties of the NW-layer differed substantially from those of crystalline Si (c-Si), making it possible to observe the interference effect in the ellipsometric spectra. This effect depends on the measurement point on the structure and it looks like as „gigantic“ (false) absorption in this range.

The absorption edge of the pseudodielectric function of NW structures was considerably moved to higher energies in comparison with c-Si. The quantity of electron transitions at 4.25 eV seems to be greater than in the c-Si case. Generally, the spectra were dramatically distorted.

4. Impact of whisker's length on optical properties of Si-NWs structures. The optical properties via whisker's length is shown in Fig.

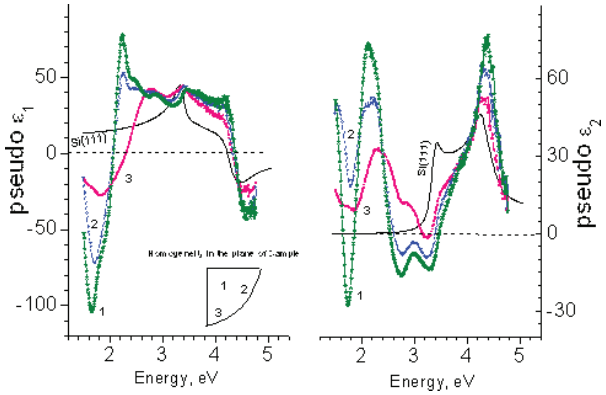

Figure 1. Spectral dependences real ε_1 and imaginary ε_2 parts of pseudodielectric function of structure Si-NWs measured in the several points as shown in insert. They demonstrate homogeneity of Si-NWs distribution in the plane of sample. Literature values of real part ε_1 and imaginary part ε_2 of Si (111) is given for comparison

2, where the 1, 2, 3 spectra corresponds to NWs structures with whisker's small length.

As a result of whisker's small length, the interband transitions at 3.43 and 4.25 eV seems to decrease abruptly and the interference effect almost disappears in the range of relative transparence of c-Si, although the optical properties of the NW layer still differed noticeably from those of c-Si. The „gigantic“ (false ghost) absorption is not appeared too.

Ellipsometric spectra of samples 1, 2, 3 are considerablely distorted in the region with strong absorption (in the vicinity of the two critical points of Si: 3.43 and 4.25 eV) as in previous case.

5. Explanation of „gigantic“ absorption.

„Gigantic“ absorption appears in that part of spectrum where reflectance of c-Si is approximately constant (0.36-0.34), as shown in Fig. 3b. Therefore this effect cannot be evoked by reflection from c-Si Presence of extremes (singularities) in imaginary part of dielectric function can be explained by relationships for interference phase of D (path-length difference), which can be equal to p or 2p in sum of partial waves reflected from substrate and from whiskers with different lengths.

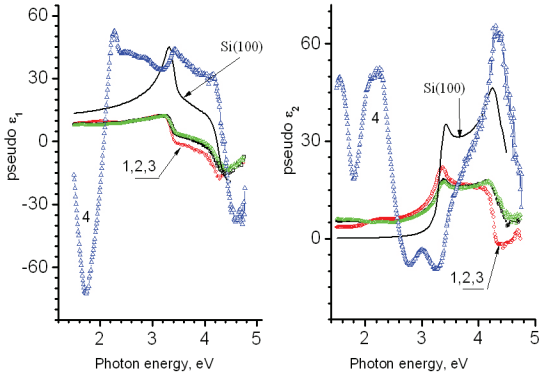

Figure 2. Ellipsometric spectra real ε_1 and imaginary ε_2 parts of pseudodielectric function of Si-NWs structure with different lengths of whiskers: 1, 2, 3–(220, 230, 240) nm, respectively; 4–(580 ÷ 990) nm. Literature values of real part ε_1 and imaginary part ε_2 of Si (100) is given for comparison.

From these conditions, wavelengths of singularities could be easily determined in according with expression (3) and taking into account an angle j_0 of oblique reflection of light. Besides in expression (3), L_1, L_2 and L_3 must be substituted for value of *d*.

$$\Delta = \frac{4\pi d \cos\varphi_0}{\lambda}, \quad \lambda_{extr} = \frac{4\pi d \cos\varphi_0}{\pi(or\,2\pi)}. \qquad (3)$$

Two most probable whisker's wavelengths L_1, L_2 and their difference are shown in Table explaining Figure 3. Wavelengths of interference l_{extr} were calculated for D=p and 2p. Their values were in close agreement with experimental extremum's positions (l) in spectrum of ε_2, all of them are shown in the same table. According to expression (3), it is quite obviously that it is impossible to register interference effect in a spectral region of UVISEL ellipsometer for 1, 2, 3 NWs structures which have whiskers of small lengths (as 0.22–0.24 mm).

Table explaining Figure 3

Whisker's length, μm	Wavelength of interference, μm		Extremum's positions (λ) in spectrum of ε_2, μm	
	λ_1 $\Delta=\pi$	λ_2 $\Delta=2\pi$		
L_1=0.99	1.39	0.699	-	0.688
L_2=0.58	0.82	0.41	0.805	0.416
$L_3= L_1- L_2$ =0.41	0.579	0.289	0.576	0.287

6. Parameters of protecting layer.

In our experiment the metal Ti layer was simultaneously deposited both onto epi-ready Si (001) wafers

and onto Si-satellite-speciment-speciment in high vacuum (10^{-5}–10^{-7}Pa), using the e-beam sputtering technique. The ~5 nm Ti layer was deposited in an ANGARA — molecular beam epitaxy unit.

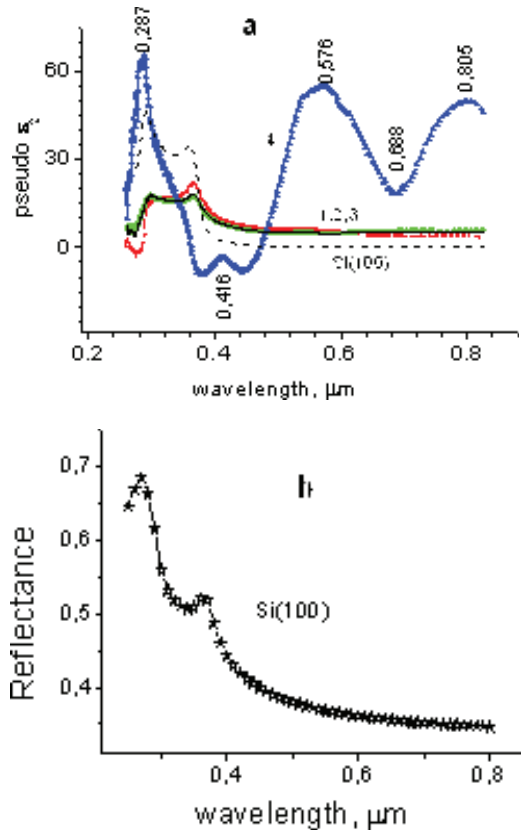

Figure 3. a) Ellipsometric spectra imaginary ε2 (l) parts of pseudodielectric function of Si-NWs structures (1, 2, 3, 4) and c-Si;
b) reflectance of c-Si in the same spectral region

The deposition rate of the metal layer was 1.0 nm/min. Plasma-chemical nitridation of Ti nano-layers for TiN nano-layers formation was carried out in plasma of nitrogen gas at pressure 0.2 Torr, with RF power 100 watt and radio frequency 13.56 MHz („MATRIX" unit) for 25 minutes at temperature 0°C by several steps cyclically: nitridation for one minute and then a cooling for 5 minutes.

Parameters of a protecting layer TiN were first studied using simplified structure of Si-satellite-speciment-speciment, as shown in Fig. 4. With the purpose of definition of properties of a finite protecting layer, three ellipsometric spectra were successively registered in terms of pseudo-dielectric functions: a) before and b) after Ti film deposition and c) after nitridation procedure, as shown in Fig. 5.

7. Modeling and calculation of parameters of satellite-speciment-speciment

Thickness of native oxide SiO_2 was found from spectra marked in figure 5 as *Si-satellite-speciment-speciment*, it was 37 Å. From the second spectra marked as *Si+Ti*, metal thickness and dielectric function of Ti were calculated; thickness of Ti was 76 Å.

In accordance with the Classical dispersion model, dielectric function is equal to the sum of high frequency value of ε_∞ and single oscillators, the number of which is determined by the number of critical points in reflectance or in a transmittance spectra. Dielectric function of transition metal Ti was approximated by a sum of four oscillators using as start spectra [12]:

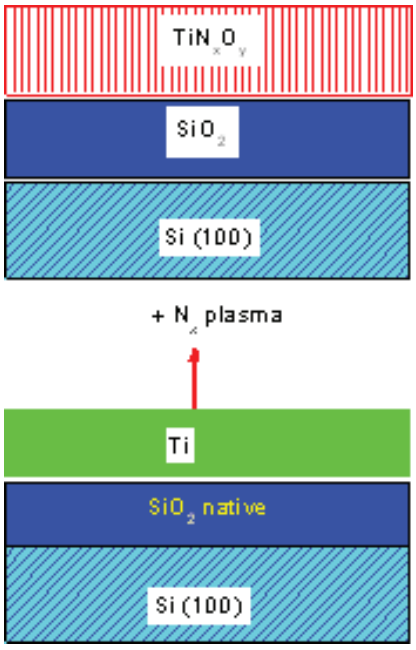

Figure 4. Structural scheme of satellite-speciment-speciment sample before and after nitridation procedure

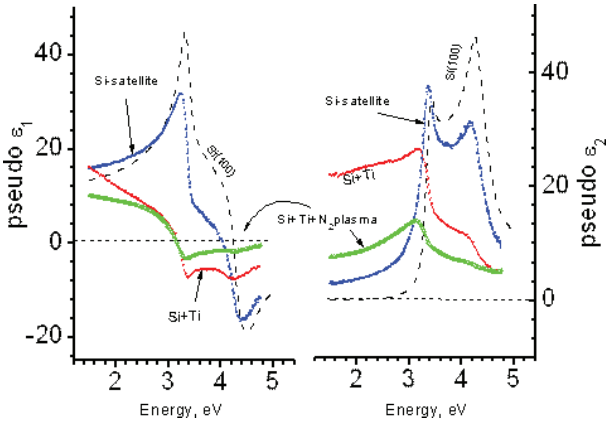

Figure 5. Ellipsometric spectra of real ε_1 and imaginary ε_2 parts of pseudodielectric function of satellite-speciment to Si-NWs structures: a) Si-satellite-speciment — before Ti metal deposition; b) Si+Ti — satellite-speciment after deposition of Ti metallic film; c) Si+Ti+N_2 plasma-satellite-speciment after nitridation procedure of metallic Ti film in nitrogen plasma. Literature values of real part ε_1 and imaginary part ε_2 of Si (100) is given for comparison

$$\varepsilon = \varepsilon_\infty + \frac{(\varepsilon_s - \varepsilon_\infty)\omega_T^2}{\omega_T^2 - \omega^2 + i\Gamma_0\omega} + \\ + \frac{\omega_P^2}{-\omega^2 + i\Gamma_D\omega} + \sum_{j=1}^{2} \frac{f_j\omega_{0j}^2}{\omega_{0j}^2 - \omega^2 + i\gamma_j\omega}, \quad (4)$$

where ε_∞ and ε_s are high frequency and static dielectric constants, respectively; Γ_0, Γ_D, γ_j are damping factors; γ_j, Γ_0, $\Gamma_D > 0$; f_j is the oscillator's strength; ω_{0j}, ω_T, ω_P are the oscillator, transverse and plasma energy in eV, respectively.

At last from the third spectra in figure 5 marked as *Si+Ti+N_2 plasma*, thickness and spectral dependence of dielectric function of a protecting film were calculated by numerical method.

Not touching special questions of solving inverse ellipsometric problem (IEP) that had already been considered by a lot of authors, for example [13–15], in this paper the algorithm of solving the IEP had consisted in determining the parameters of two layers: a) silicon dioxide and titanium and b) silicon dioxide and titanium oxynitride. For minimizing the error function of χ^2 (which was defined by the difference between the measured value and the value calculated according to proposed model (figure 4)), we used the Marquardt-Levenberg method:

$$\chi^2 = \frac{1}{2N}\left\{\sum_i^N \mathrm{Re}\left[\frac{\varepsilon_{measur}(\omega) - \varepsilon_{calcul}(\omega)}{\alpha}\right]^2 + \right. \\ \left. + \sum_i^N \mathrm{Im}\left[\frac{\varepsilon_{measur}(\omega) - \varepsilon_{calcul}(\omega)}{\beta}\right]^{-2}\right\}, \quad (5)$$

where *a* and *b* are the weight factors.

The thickness of film was 141 Å. Thus, 76 Å of metallic titanium were converted into 141 Å oxynitride TiNxOy, optical properties of which are similar to film properties described in [16–18] and shown in Fig. 6. It needs to note that metallic film disappeared completely after nitridation procedure as it followed from calculations.

8. Impact of protecting layer on optical properties of NWs structures grown by MBE

Structure of Sample: Si (111) (Ocmetic)/70 Å of MBE-Si, deposited at 200° C/1100 Å of MBE-Si, deposited at 550°C/20 Å of Au/5400 Å of Si-whiskers is schematically shown in figure 7 before deposition of titanium film and after nitridation procedure.

Sequence of experimental ellipsometric spectra of Si-NWs structures for whiskers with great lengths are shown in figure 8. In the same figure the spectra of e (E) of c-Si (100) are given for comparison. Spectra marked as *Si-whisker* are given for Si-NWs structures as grown; spectra marked as *Si-whisker+Ti* are given for Si-NWs structures after deposition metallic film of titanium and spectra marked as *Si-whisker+Ti+N_2plasma* are given for Si-NWs structures after treatment in nitrogen plasma. Because all treatments were simultaneously carried out both at satellite-speciment and at Si-NWs structures, that parameters of deposited and protecting layers were the same in both cases. The impact of deposited Ti film as well as the impact of nitridation on ellipsometric spectra were enormous. It needs to note one very significant detail: energy position of interference peaks in the range of 1.5–2.6 eV had not been almost displaced. These phenomena tell us in favor of suggested interpretation of „gigantic" absorption. The magnitude of interference peak is greater if reflectivity of the deposited film is larger; it was the greatest for metallic Ti film.

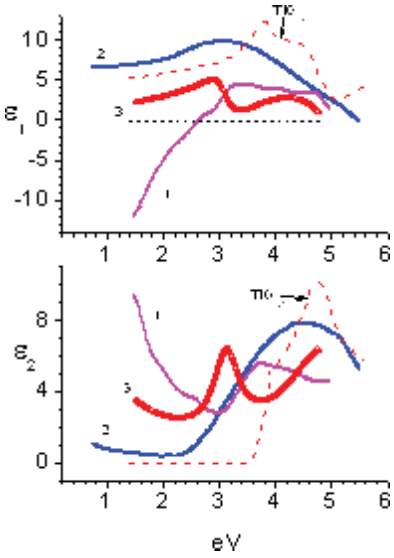

Figure 6. 3)–Optical properties of film TiNxOy generated by nitridation procedure of metallic Ti. Dependences of ε(E) of films produced by other methods: 1)–[16, 17] and 2)–[18 (for gas ratio $PN_2/(PN_2 + PO_2)$=0.78)]; spectra of TiO_2 [19] are given for comparison

It is necessary to notice that the creation of an optical model for NWL is a very difficult task which is waiting for solution. However, to explain above mentioned effects observed in the spectra in figure 8 by means of calculation, the dielectric function of just the NWs layer should be described by some model and then the parameters of model could be obtained from ellipsometric spectra. The effective medium approximation (EMA) based on the theory of additivity of polarizability for a mixture of several components (in volume fractions) is used as a rule to describe the dielectric function of a non-homogeneous layer.

In our cases experimental structures had, on one hand, a large length of NWs ($L^3 \lambda$), and on the other hand, small their volume fraction in the layer.

Unfortunately, under these conditions EMA is not applicable for modeling a layer similar to the NWL.

8. Conclusions

The ellipsometric spectra of NW structures in the range 1.5–4.77 eV differ from those of c-Si, making it possible to inspect such structures for planar uniformity and to check the reproducibility of NW structures grown by various methods because the height and distribution

of whiskers over the substrate noticeably impact on ellipsometric spectra. Thus immediately after the recording of the spectra, spectroscopic ellipsometry can be profitably employed as non-destructive, non-disturbing technique, without modeling and making any calculations. "gigantic" absorption was easily explained by a change of path-length difference of reflected light.

9. Acknowledgments

The authors are grateful to Medvedev A. S. for the samples and fruitful discussions.

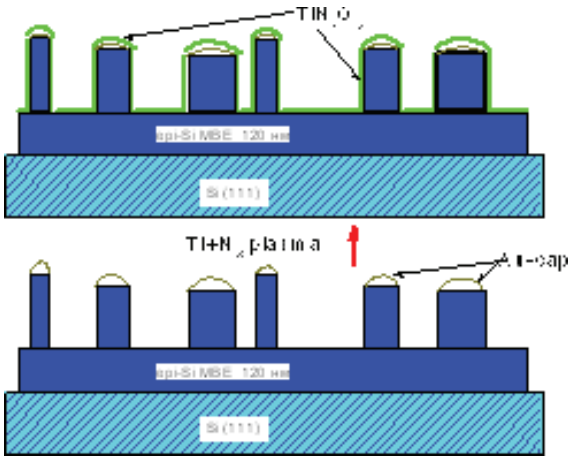

Figure 7. Structural scheme of Si NWs-structure before and after nitridation procedure

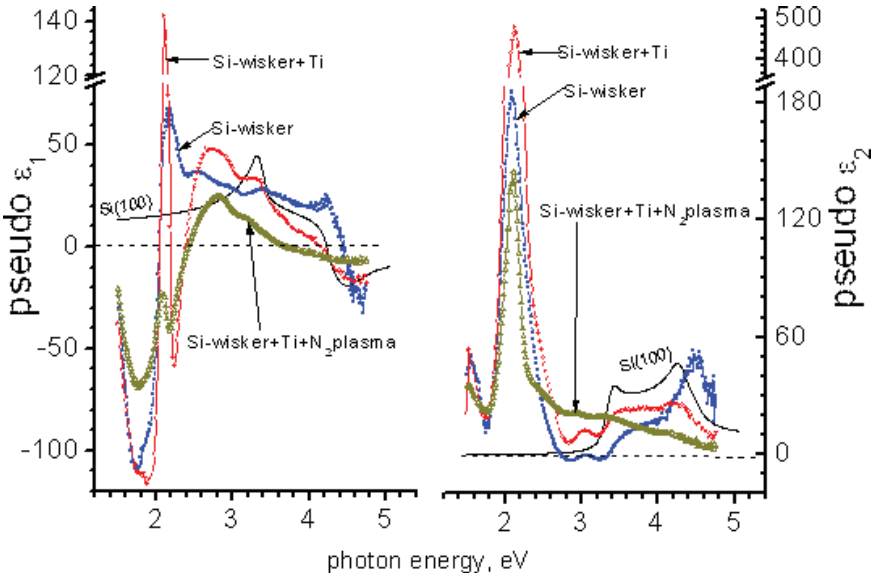

Figure 8. Spectral dependences of optical properties (real ε_1 and imaginary ε_2 parts of pseudodielectric function): a) of Si-NWs structure with great length of whiskers (580¸990 nm); b) of the same Si-NWs structures metallized by Ti; and c) after treatment in nitrogen plasma. Literature values of real part ε_1 and imaginary part ε_2 of Si (100) is given for comparison

Bibliographical list

1. Liu J.L., Cai G.L., Jin S.G., Thomas S.G. and Wang K.L. 1999 *J. Cryst. Growth* **200**106

2. Zhang Y., Zhang Q., Wang N., Yan Y., Zhou H. and Zhu J. 2001 *J. Cryst. Growth* **201**185

3. Schubert L., Werner P., Zakharov N.D., Gerth G., Kolb F.M., Long L. and Gosele U. 2004 *Appl. Phys. Lett.* **84**4968.

4. Zakharov N.D., Werner P., Gerth G., Schubert L., Sokolov L. and Gosele U., 2006 *J. Cryst. Growth* **290**6.

5. Zakharov N., Werner P., Sokolov L. and Gosele U. 2007 *Physics* E*: Low-dim. Sys. Nano.* **37**148.

6. Svitasheva S. N., Sokolov L. V., Zakharov N. D. and Werner P 2007 *Proc. ICSE-4 (Stockholm)*.

7. Naumova O.V., Nastaushev Yu.V., Svitasheva S.N., Sokolov L.V., Zakharov N.D., Werner P., Gavrilova T.A., Dultsev F.N. and Aseev A.L. — Nanotechnology —2008. — Vol. **19**, 225708.

8. Nastaushev Yu.V., Svitasheva S.N., Sokolov L.V., Werner P., Zakharov N.D., Gavrilova T.A., Naumova O.V., and Aseev A.L. Proceedings of 14th International Symposium on Nanostructures Physics and Technology, 2006, St. Petersburg, Russia.

9. Svitasheva S.N., Gutakovskiy A.K., Nastaushev Yu.V., MRS spring meeting 2008, San Francisco CA, USA H4.42.

10. Naumova O.V., Nastaushev Y.V., Svitasheva S.N., Sokolov L.V., Werner Peter, Zakharov N.D., Gavrilova T.A., Dultsev F.N., Aseev A.L. — INST PHYS CONF SER -2007- Vol. **893**, № 1, p. 7390.200.67; Proceedings of 28th International Conference on the Physics of Semiconductors, 2006, Austria, Vienna.

11. Azzam R. M. A. and Bashara N. M. 1977 *Ellipsometry and Polarized Light* (Amsterdam: North-Holland).

12. Johnson P.B., Christy R.W., Physical Review B, 1974, V. **9**, No.12, P. 5056–5070.

13. Svitasheva S.N., DAN SSSR **318** (5), 1154 (1991).

14. Svitasheva S.N. Avtometriva. No. 4. 119 (1996) [Optoelectr. Instrum. Data Process. No. 4. 108 (1996)].

15. Voskoboinikov Yu.E., Petukhova E.V., and Svitasheva S.N., Avtometriva, No. 4, 110 (1996) [Optoelectr. Instrum. Data Process. No. 4, 99 (1996)].

16. Langereis E., Heil S.B. S., van de Sanden M.C. M., and Kessels W.M. M., *J. Appl. Phys*. **100**023534 (2006).

17. Langereis E., Heil S.B. S., van de Sanden M.C. M., Kessels W.M. M. P*hys. Stat. Sol.* ***(c)*** **2**, 3958 (2005).

18. Mohamed S.H., Kappertz O., Ngaruiya J.M., Niemeier T., Drese R., Detemple R., Wakkad M.M., Wuttig M. *Phys. Stat. Sol.* ***(a)*** **201**, 90 (2004).

19. Jellison G.E., Jr., Boatner L.A., and Budai J.D., Jeong B.S. and Norton D.P. *Journal of Applied Physics*. — Vol. 93, Number 122003.